HIGH-LUMINOSITY LHC COLLIMATION PERFORMANCE WITH MACHINE ERRORS AND DURING FAST FAILURES*

A. Donadon Servelle†, R. Bruce, R. Cai, B. Lindström, S. Redaelli
European Organization for Nuclear Research, CERN, Geneva, Switzerland

Abstract

Due to the increase in stored beam energy to almost 700 MJ in the High-Luminosity LHC, the safe handling of any beam losses by the collimation system is more critical than at the LHC, designed for 362 MJ per beam. The cleaning performance of the collimation system could be negatively impacted by imperfections and errors in machine elements. Errors in collimator jaw positions or angles, optics and orbit, and machine aperture imperfections can produce increased losses at sensitive locations. In addition, fast failure scenarios, such as asynchronous beam dumps, could cause large single-turn losses, posing a potential threat to different machine elements, including collimators. In this paper, simulations with Xsuite were performed to assess the performance of the collimation system, comparing results for an ideal machine against scenarios including imperfections, and predicting the resulting beam losses around the ring due to an asynchronous beam dump.

INTRODUCTION

Various imperfections can affect the performance of accelerators. While the design performance of the collimation system in protecting the accelerator from beam losses is initially assessed using simulations in an ideal lattice, it is important to quantify the impact of realistic errors. In this context, understanding how imperfections degrade the cleaning efficiency and affect loss distributions is a key ingredient for a robust machine protection strategy.

Previous studies have highlighted the sensitivity of the LHC collimation system [1–3] to imperfections in both collimator settings and machine aperture [4,5]. Building on these results, the present work focuses on errors in the upgraded High-Luminosity LHC (HL-LHC) [6] on collimator jaw tilts, transverse offsets, and half-gaps, as well as offsets of the magnet apertures. For each collimator jaw and each error source, values are sampled from a normal distribution, with the widths derived from measurements [4]. By repeating the simulations for many random seeds, the variation of the main observables for collimation performance, namely the local cleaning inefficiency and the losses on tertiary collimators (TCTs) have been studied.

In addition, the LHC is exposed to a range of failure scenarios in which beam losses can become critical. Examples include injection and extraction kicker failures, beam instabilities, and failures of magnets or power supplies. Among these, failures of the beam extraction system are particularly critical, as they can generate large single-turn losses that may damage sensitive equipment, e.g. magnet apertures or tungsten-based collimators such as TCLAs (shower absorbers) and TCTs.

During a normal beam extraction, 15 horizontal kicker magnets, called MKDs, rise from zero to full field synchronously during a 3 µs abort gap (about 3% of the revolution period) with no beam passing (see Fig. 1). An asynchronous beam dump (ASDs) occurs when all MKDs fire synchronously outside of the abort gap, hence giving intermediate kicks to passing bunches that risk to be deflected onto sensitive elements. In a single-module pre-fire (SMPF), one of the 15 MKDs fires with beam passing, and the rest of the kickers re-trigger shortly after. This is potentially more critical than an ASD as more bunches can be mis-kicked with the effect depending on which module fires first.

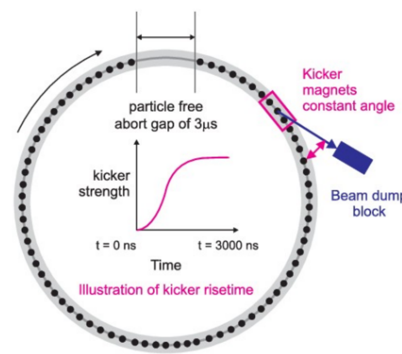

Figure 1: Illustration of ASD.

In the following two sections, these studies are presented in detail and summarised in the HL-LHC context.

MACHINE IMPERFECTIONS

The simulations were performed with Xsuite [7], using its collimation package Xcoll [8] coupled with the default scattering routine *everest* [9]. Xsuite also features coupling to FLUKA [10–12], or Geant4 [13, 14], for collimator simulations, but for this study *everest* was chosen due to its simpler and faster model.

For the simulations, the optics correspond to the HL-LHC round optics configuration v1.6, including a new high-β optics in the collimation insertions (insertion region 3 - IR3, and insertion region 7 - IR7) and $\beta^* = 15$ cm, relaxed collimators settings as defined in [15], and the following rms values for the normal distributions of the error parameters:

- Collimator tilts: 200 μrad
- Collimator offsets: 180 μrad
- Error on collimator centring: 0.17 sigma

* Research supported by the HL-LHC project.
† andre.donadon.servelle@cern.ch

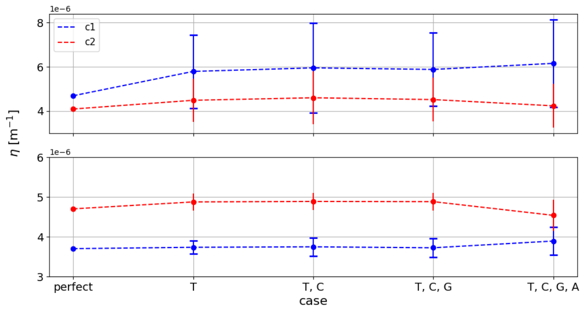

Figure 2: Cleaning inefficiency comparison in IR7 DS clusters c_1 and c_2 clusters between perfect machine and various configurations of errors. B1H and B1V upper and lower plot respectively.

– Dipoles aperture offset: x-offset = 2×10^{-3} mm and y-offset 1.5×10^{-3} mm

Simulations were done using a direct halo hitting the primary collimator in either the horizontal or vertical plane as in [5]. Both beams (B1 and B2) were simulated. Several sets of simulations were done, starting from a perfect machine without imperfections, and then introducing one error source at a time to disentangle their effects. For each set of error sources, 100 different random seeds resulting in different imperfect machines were sampled, and 100 primary halo particles were simulated for each machine. The results were analysed in terms of losses on TCTs and the average cleaning inefficiency (η) in the clusters of losses in the dispersion suppressor(DS) downstream of IR7 as in [5]. For each set of errors, the average and standard deviation over the random seeds were calculated.

Figures 2 and 3 show the results for the cases without imperfections, with just tilts (T), tilts and offsets (TC), tilts, offsets and gaps (TCG), and all error sources combined including also aperture offsets (TCGA), for η and TCT losses. Since the B2 results are qualitatively equivalent, only B1 is shown here. Based on the calculations presented in [15], the requirement is a $\eta \lesssim 5 \times 10^{-5} m^{-1}$ and TCT losses $<< 10^{-2}$. Although η and TCT losses increase with imperfections compared to the perfect machine, the values remain within acceptable limits for all cases, with more than one order of magnitude of margin below the plastic deformation threshold.

EXTRACTION FAILURES

The simulations use the same HL-LHC v1.6 optics, with relaxed collimator settings, and both beams are simulated. The workflow consists of simulating several Gaussian bunches separately, considering only those bunches that are affected by the rising kicker field and kicked at amplitudes of potential concern for the aperture. This corresponds to a specific time window, since initially the kick introduces only small perturbations to the bunches, which are then fully deflected on their second turn, while at later times the MKDs become strong enough to kick the bunches cleanly to the dump channel without any aperture losses. To define the strength of the MKDs, measurements from actual accidental firings were used, as reported in Ref. [3, 16]. In total, about 60 bunches were simulated, with 5×10^6 macroparticles per bunch. Fig. 4 shows the full lossmap produced by summing the losses over all bunches and normalising to the actual expected bunch intensity of 2.2×10^{11} protons/bunch.

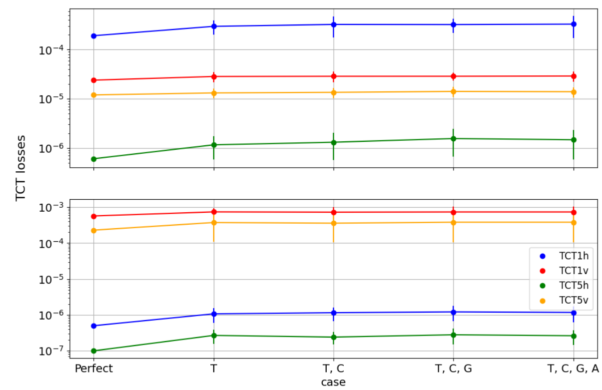

Figure 3: TCTs in IR1 and IR5 losses comparison between perfect machine and various configurations of errors. B1H and B1V upper and lower plot respectively.

The main objective of this study is to quantify the safety margins for the collimator half-gaps, which are already safe in this nominal configuration, as will be shown in the results below. In this context, the simulations aim at assessing the sensitivity of the system to imperfections by modifying the relative margins between collimators and investigating how large these changes can be before the losses become relevant. A critical input to identify if unsafe conditions occur is the damage limit of collimators and other affected elements in terms on number of protons lost. Reference [17] indicates that to avoid plastic deformation of the tungsten, these losses must remain $\lesssim 5 \times 10^9$ protons.

Among the collimator hierarchy, the TCDQs and TCSPs are the primary protection devices in the dump region, positioned to intercept the beam in the event of an asynchronous beam dump and thereby shield the downstream aperture and sensitive elements. Additionally, the tungsten-based TCTs and TCLAs are relatively non-robust and must be protected from large single-turn losses that could lead to plastic deformation or damage. A dangerous situation can therefore arise either if the TCDQs/TCSPs are too far away from the beam, or if the sensitive tungsten collimators TCTs and TCLAs come too close to the beam halo.

To prove these two regimes, three different scans were performed: the TCDQs/TCSP were opened in steps of 2σ, while the TCTs and TCLAs were closed in steps of 1σ. This scan strategy allows us to systematically evaluate how the safety margins change with respect to both the protection devices in the dump region and the tungsten-based collimators, and to identify the operation windows in which the system remains robust against fast failure scenarios.

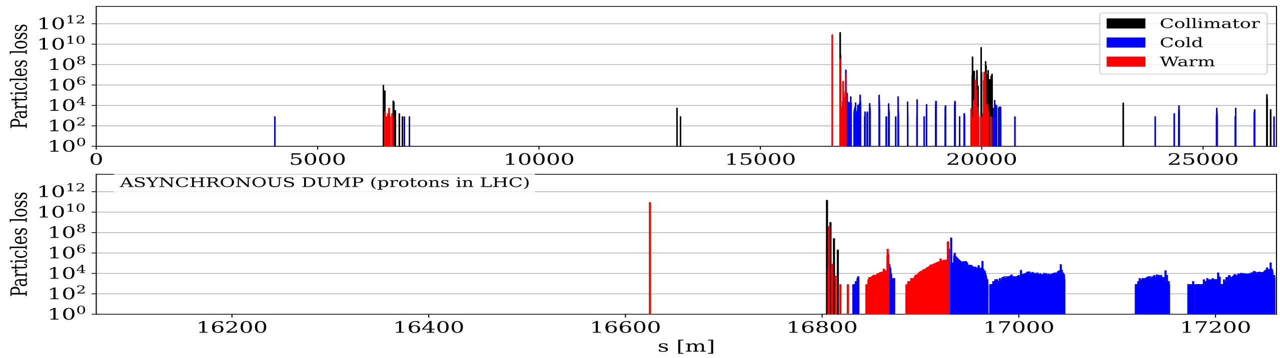

Figure 4: Lossmap for a B1 ASD at 7 TeV. HL-LHC v1.6 round optics with 15 cm β^* and relaxed collimator settings.

Figures 5-7 show, respectively, the losses on various collimators in the scans of TCDQ, TCLAs and TCTs, for a perfect optics without errors. The Beam 2 results are more critical since Beam 1 has IR7 right after the dump in IR6, allowing for a better energy deposition in this case. Therefore, only Beam 2 is presented here. In all the figures, only the collimators with highest losses in each family are included, these being the primaries (TCPs), secondaries (TCPs), TCLAs and TCTs. The least critical case is that of the TCTs. Starting from nominal settings of 11.4 σ, the horizontal TCT in IR5 approaches the plastic deformation threshold at 3-4 σ tighter setting. For the TCLAs, the results indicate that these collimators can be safely closed down by about 2.5–3 σ. In contrast, opening the TCDQs impacts several downstream collimators, including the TCSGs and TCLAs. Since the latter are tungsten-based, the limiting factor in this scan is the load on the TCLAs, in which case the damage limit is reached at a 2.5 σ more open TCDQ setting.

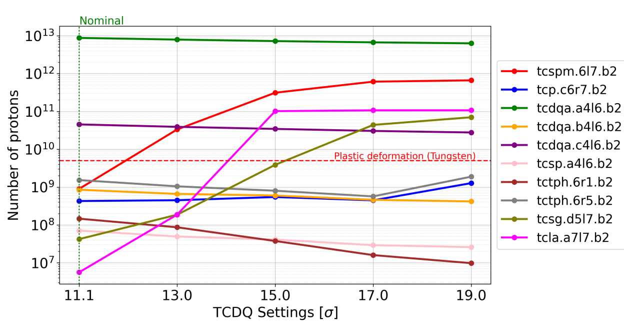

Figure 5: Proton losses on various collimators as a function of TCDQs/TCSP half-gap opening, for a B2 SMPF at 7 TeV.

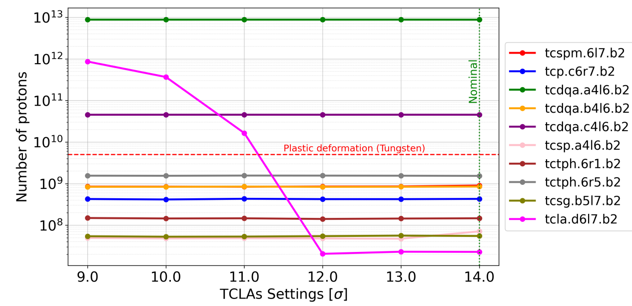

Figure 6: Proton losses on various collimators as a function of TCLAs half-gap closing, for a B2 SMPF at 7 TeV.

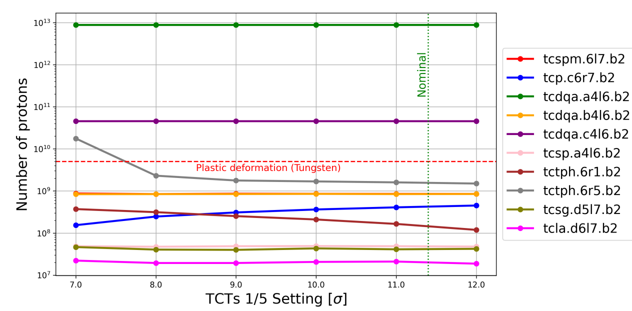

Figure 7: Proton losses on various collimators as a function of TCTs half-gap closing, for a B2 SMPF at 7 TeV.

In the context of fast failure scenarios for a perfect machine, the analysis of a single-module pre-fire of one extraction kicker confirms that the settings of tungsten-based collimators such as TCLAs and TCTs are robust with sufficient safety margins. For the TCTs, the jaws can be closed by up to about 3-4 σ from their nominal setting before expected beam losses during the studied failure reaches the plastic deformation limit. The TCLAs can be closed down to 2.5-3 σ without exceeding the same limit. If the TCDQs are opened beyond 2.5 σ, losses on TCLAs become too high. The results provide clear guidance for defining safe operational settings for the collimators in the HL-LHC, in the presence of realistic machine errors. Future work could extend the study to include errors in the ASD, additional failure types and different HL-LHC optics configurations, in order to further refine the robustness of the collimation system and to support the design of more flexible, yet safe, high-luminosity operation scenarios.

CONCLUSIONS AND OUTLOOK

The simulations presented in this work show that, even when realistic machine imperfections are taken into account, the HL-LHC collimation system operates well within the required safety margin for both cleaning inefficiency and TCT losses. For the imperfection scenarios considered, the average values over many imperfection seeds remain below the reference limits, with the worst case configuration still reasonably below the critical thresholds. This indicates that, for normal operation, the expected background from tertiary collimators should remain low for the HL-LHC experiments.

REFERENCES

[1] O. S. Brüning *et al.*, "LHC Design Report V.1 : the LHC main ring", *CERN-2004-003-V1*, 2004.

[2] R. Assmann, F. Schmidt, and F. Zimmermann, "Equilibrium beam distribution and halo in the LHC", *Proc. of the European Particle Accelerator Conf. 2002, Paris, France*, p. 1326, 2002. http://accelconf.web.cern.ch/e02/PAPERS/WEPLE048.pdf

[3] R. Bruce *et al.*, "Reaching record-low β^* at the CERN Large Hadron Collider using a novel scheme of collimator settings and optics", *Nucl. Instrum. Methods Phys. Res. A*, vol. 848, pp. 19–30, Jan. 2017. doi:10.1016/j.nima.2016.12.039

[4] C. Bracco, "Commissioning Scenarios and Tests for the LHC Collimation System", Ph.D. thesis, EPFL Lausanne, 2008.

[5] R. Bruce *et al.*, "Simulations and measurements of beam loss patterns at the CERN Large Hadron Collider", *Phys. Rev. Spec. Top. Accel. Beams*, vol. 17, p. 081004, 2014. doi:10.1103/PhysRevSTAB.17.081004

[6] I. B. Alonso *et al.*, *High-Luminosity Large Hadron Collider (HL-LHC): Technical design report*. Geneva: CERN, 2020. doi:10.23731/CYRM-2020-0010

[7] G. Iadarola *et al.*, "Xsuite: an integrated beam physics simulation framework", in *JACoW HB 2023*, Geneva, Switzerland, TUA2I1, 2024. doi:10.18429/JACoW-HB2023-TUA2I1

[8] F. F. Van der Veken, "Introducing xcoll: a streamlined approach to collimation and beam loss simulations using xsuite", https://indico.gsi.de/event/19249/contributions/82656/attachments/48844/70973/ICAP_Xcoll.pdf, presented at ICAP'24, Seeheim, Germany, October 2024, 2018,

[9] F. Van der Veken *et al.*, "Recent Developments with the New Tools for Collimation Simulations in Xsuite", in *JACoW HB 2023*, pp. 474–478, 2024. doi:10.18429/JACoW-HB2023-THBP13

[10] C. Ahdida *et al.*, "New capabilities of the FLUKA multi-purpose code", *Frontiers in Physics*, vol. 9, 2022. doi:10.3389/fphy.2021.788253

[11] "Fluka website", https://fluka.cern/, Accessed: 2021-11-30, 2022,

[12] G. Battistoni *et al.*, "Overview of the FLUKA code", *Ann. Nucl. Energy*, vol. 82, pp. 10–18, 2015. doi:10.1016/j.anucene.2014.11.007

[13] S. Agostinelli *et al.*, "Geant4 - a simulation toolkit", *Nucl. Instrum. Methods Phys. Res., Sect. A*, vol. 506, pp. 250–303, 2003. doi:10.1016/S0168-9002(03)01368-8

[14] J. Allison *et al.*, "Recent developments in Geant4", *Nucl. Instrum. Methods Phys. Res., Sect. A*, vol. 835, pp. 186–225, 2016. doi:10.1016/j.nima.2016.06.125

[15] Donadon Servelle, A. and others, "An evaluation of collimation settings for the High Luminosity LHC baseline", in *Proc. IPAC'25*, Taipei, Taiwan, pp. 2532–2535, Nov. 2025. doi:10.18429/JACoW-IPAC2025-THPB015

[16] R. Bruce, R. W. Assmann, and S. Redaelli, "Calculations of safe collimator settings and β^* at the CERN Large Hadron Collider", *Phys. Rev. Spec. Top. Accel. Beams*, vol. 18, no. 6, p. 061001, Jun. 2015. doi:10.1103/PhysRevSTAB.18.061001

[17] E. Quaranta *et al.*, "Modeling of beam-induced damage of the LHC tertiary collimators", *Phys. Rev. Accel. Beams*, vol. 20, no. 9, p. 091002, Sep. 2017. doi:10.1103/PhysRevAccelBeams.20.091002